

# Spin transference and magnetoresistance amplification in a transistor

H. Dery,\* L. Cywiński, and L. J. Sham

*Department of Physics, University of California San Diego, La Jolla, California, 92093-0319*

(Dated: May 1, 2019)

A current problem in semiconductor spin-based electronics is the difficulty of experimentally expressing the effect of spin-polarized current in electrical circuit measurements. We present a theoretical solution with the principle of transference of the spin diffusion effects in the semiconductor channel of a system with three magnetic terminals. A notable result of technological consequences is the room temperature amplification of the magneto-resistive effect, integrable with electronics circuits, demonstrated by computation of current dependence on magnetization configuration in such a system with currently achievable parameters.

Giant magnetoresistance effect has been discovered in heterostructures of ferromagnetic and paramagnetic metal layers [1, 2]. Similar effect has been observed in magnetic tunnel junctions [3]. Applications in the spin valve configuration has given rise to important products such as hard disk read-heads and magnetic memories [4]. Research into spin polarized currents in semiconductors leads to the new field of semiconductor spintronics [5, 6] with promise of increased logic functionality of electronic circuits and integration with non-volatile magnetic memory. While room temperature injection from a ferromagnet via a tunnel barrier into a semiconductor has produced reasonable current spin polarization [7, 8, 9, 10], the magneto-resistive effect in a semiconductor spin valve with ferromagnetic metal contacts is predicted to be small [11, 12]. In order to introduce additional control over the spin-polarized carrier flow, a number of semiconductor-based spin-transistors have been proposed [13, 14, 15, 16, 17], using ideas such as Rashba effect, effective spin reflection, half-metallic ferromagnets, or minority carrier action in junctions with a magnetic semiconductor.

In this Letter we present an electrical means of expressing the spin effects, rather than optical means [18, 19]. We study the diffusive spin currents of a non-magnetic semiconductor (SC) with three ferromagnetic metal (FM) terminals, each capable of injecting or extracting spin-polarized currents. The currents flowing between the contacts depend on the alignment of their magnetizations. The magneto-resistive (MR) effect is defined as a relative change of the current upon flipping of one of the magnetization vectors. In the diffusive regime considered here, the MR effect comes from spin accumulation in the semiconductor due to the spin selectivity of the contacts. The profiles of non-equilibrium spin densities in the semiconductor depend on the magnetic configuration, and the resulting different diffusion currents are the cause of MR. Using more than two terminals provides the capability of transference of spin effects from one controlled diffusion region to another. This transference under voltage and magnetization control will be shown to lead to amplification of the magneto-resistive effect. This control provided by a third conducting and

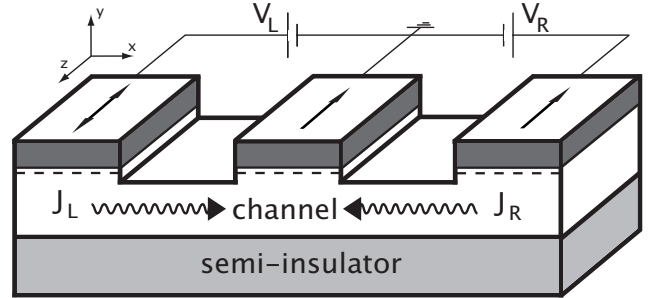


FIG. 1: A schematics of the proposed three-terminal device. The channel indicates the current flow region of  $n$ -doped semiconductor grown on top of an insulating substrate.

biased terminal is in contrast to the “nonlocal” spin valve geometry [20, 21], where the additional contact is a floating voltage probe.

An illustrative application of these ideas is a device we term magnetic contact transistor (MCT), shown in Fig 1. The principle behind such a system is analogous to the familiar bipolar transistor. Here the two spin diffusion channels whose populations can change by spin-flip take the place of electrons and holes whose populations are changed by recombination. In the latter case, the transistor action results from attaching two p-n diodes back to back into a pnp or npn structure, in which the common base width must be smaller than the recombination diffusion length. A longer base would beget two uncoupled diodes devoid of amplification effects. The two-terminal device in spintronics is a spin-valve, in which the current depends on the relative magnetization directions of two magnetic contacts. By connecting two spin valves with a common source terminal (the middle contact in Fig. 1), whose width is smaller than spin-diffusion length  $L_{sc}$ , we create a system capable of amplifying the MR effect of each spin valve. In contrast to the bipolar transistor, the spin current is driven by spin diffusion rather than charge diffusion. In addition to the current control by applied voltages as in the conventional transistor, this spin transistor has control of the spin components by the magnetization configurations of the ferromagnetic electrodes. One strategy in amplifying the MR effect is based on the

ability to use the voltage adjustment to yield a zero or near zero current in one magnetic configuration of the ferromagnetic electrodes, and the ability to produce an easily measurable current at the same voltage arrangement by changing the magnetic configuration. The former is simple circuit theory and requires no spin physics but the latter is a result of intricate spin transport physics in the transistor configuration. In our scheme, it requires the coupling of three contacts via spin currents, equivalent to coupling spin transport of two spin valves. The ratio of the “on” current to the “off” current will be shown below to be robust against electrical noise and to decay with increasing width of the middle contact or, equivalently, the distance between two spin valves beyond the spin diffusion length, indicative of the essential role of spin.

The system shown in Fig. 1 is a planar structure. Low mesas beneath the FM terminals are heavily doped, making the Schottky barriers thin (<10 nm). As an illustration here, we let the left drain (L) be a “soft” magnetic layer whose magnetization can be easily flipped. The middle source (S) and the right drain (R), are magnetized in the same direction. The P and AP configurations denote, respectively, the L magnetization parallel and antiparallel to that of the S and R. The currents  $J_{L(R)}$  are flowing in the L (R) part of the channel, and are measured in the L(R) contacts, which are kept at separately controlled voltages  $V_{L(R)}$ . The required magnetic properties of contacts can be achieved either by pinning the magnetization of middle and right terminals, or by exploiting the contacts’ magnetic shape anisotropy, in order to manipulate their coercivities. The magnetization of the left drain can be controlled by external magnetic field (then our system works as a sensor of  $B$  field), or by a field created by a pickup current in a wire above the contact. Analogously to CMOS transistors, the MCT has the capacity for digital operation that can be used to trigger a pickup current of another MCT, thus transferring the information from one magnet to another, leading to a new paradigm of computation [4, 22].

We assume the system to be homogeneous in the  $z$  direction (see Fig. 1) and consider two-dimensional spin diffusion in the semiconductor:

$$\nabla^2 \mu_s(x, y) = \frac{\mu_s(x, y) - \mu_{-s}(x, y)}{2L_{sc}^2}, \quad (1)$$

where  $\mu_s$  is the spin dependent electrochemical potential with  $s=\pm$  denoting the spin species, and the spin diffusion length  $L_{sc} = \sqrt{D\tau_{sp}}$ , where  $D$  is the diffusion constant and  $\tau_{sp}$  is the spin relaxation time. This equation is well known for paramagnetic metals [23], and holds for non-degenerate semiconductors considered here when the electric field is small [24]. This condition is fulfilled here because of the presence of highly resistive barriers at the FM/SC interface. In the following calculations the electric driving force on the current is shown to have

negligible influence on spin diffusion. Due to vastly different resistances in metals and semiconductors, we can neglect the spin and spatial dependence of the electrochemical potential in the ferromagnets and replace  $\mu_s^{FM}$  by a constant given by the bias voltage. Thus, we only need to solve the diffusion equation inside the semiconductor channel. We neglect interfacial spin scattering and use Ohm’s law across the contacts, so that the boundary conditions are:

$$ej_s^i = \frac{\sigma_{sc}}{2} (\hat{n} \cdot \nabla \mu_s) = \begin{cases} -G_s^i (eV^i + \mu_s), & \text{contacts} \\ 0, & \text{otherwise,} \end{cases} \quad (2)$$

where  $j_s^i$  denotes the spin  $s$  current through the  $i^{th}$  barrier interface,  $\sigma_{sc}$  the semiconductor conductivity,  $\hat{n}$  the outward interface normal and  $G_s^i$  the spin-dependent barrier conductance. The spin-selective properties of the tunneling barrier ( $G_+ \neq G_-$ ) dominate the spin injection physics [25]. This approach is valid for contacts without depletion beyond the thin doped tunneling barrier [26]. Elsewhere we will derive from the 2D diffusion an effective 1D formalism for the lateral spin transport inside a thin layer, with finite-sized metal contacts on top of it. The calculations presented below were done with both methods giving essentially the same results. Confining the spatial extent of spin accumulation to the terminals’ footprint is optimal for MR amplification. It is achieved by etching away the semiconductor peripheries in Fig. 1, or by selectively doping the channel with ion implantation.

The barrier conductances  $G_s$  have been calculated for Fe/GaAs system in the simple single-band effective mass model [27]. We have assumed triangular Schottky barriers of  $\sim 7$  nm thickness. At low applied voltages we obtain the conductances of the order of  $10^2$  ( $10^3$ )  $\Omega^{-1}\text{cm}^{-2}$  for reverse (forward) bias. The ratio of reverse to forward bias conductance  $f$  is taken to be 0.5, a value poorer than the theoretical estimate of 0.2. The ratio of spin-up to spin-down conductance is  $G_+/G_- \simeq 2$ . The corresponding spin-injection efficiency coefficient  $\alpha = (G_+ - G_-)/(G_+ + G_-)$  is 30% as seen in circular polarization degree of spin light emitting diodes [7, 8]. The spin selectivity of the interface is governed by the ratio of Fermi velocities for up and down spins in Fe. While this simple model lacks details of the atomic structure of the interface [28], both the  $G_+/G_-$  ratio and the orders of magnitude of  $G_s$  are in agreement with the experimental results.

It is instructive to look at the behavior of one half of the semiconductor channel decoupled from the other as a two-terminal spin valve. We define  $MR = (J^P - J^{AP})/J^P$ , with  $J^P$  ( $J^{AP}$ ) denoting the total current through the structure for parallel (antiparallel) alignment of magnetizations of the two terminals. We consider a GaAs layer at room temperature with a conservative value of  $L_{sc} = 1 \mu\text{m}$ . It corresponds to a spin-independent mo-

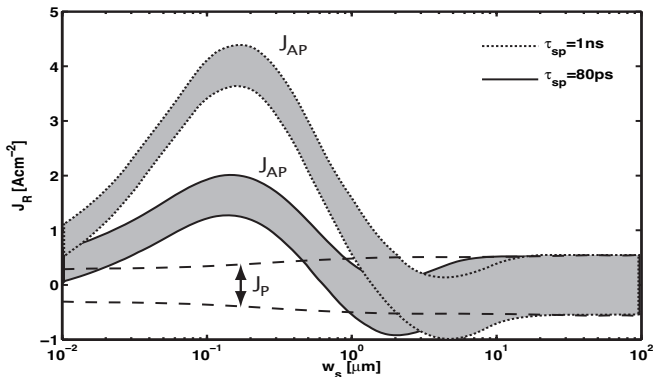


FIG. 2: Right drain current density versus source width for the left drain magnetization parallel (P) and antiparallel (AP) to the other two magnets.  $V_L = 0.1V$  and  $V_R$  is adjusted for each  $w_s$  so that  $J_R^P = 0$ . Upper and lower curves of each set show the current densities for  $V_R \pm 0.2$  mV. The dashed lines are the values for  $J_R^P$  around zero current. The solid and dotted lines show the currents for  $J_R^{AP}$  for two different spin-flip times. The drain width, separation between the contacts and the channel thickness are  $w=d=2h=0.2$   $\mu\text{m}$ .

bility of  $5000 \text{ cm}^2/(\text{Vs})$  and spin relaxation time  $\tau_s=80$  ps in the non-degenerate regime at room temperature [29]. The free carrier concentration is  $n=4 \cdot 10^{15} \text{ cm}^{-3}$ . The lower spin conductance of the forward-biased barrier  $G_b = 1000 \Omega^{-1} \text{ cm}^{-2}$ . The dimensions are the following: the contact width  $w$  and the separation between the contacts  $d$  are both 200 nm, and the thickness of the semiconductor channel is 100 nm. For these parameters we obtain the spin-valve MR  $\approx 3\%$ . Such a small effect is hard to measure and useless for applications. The weak effect can be understood from a simplified 1D transport picture where the analytical solutions are easily available [11, 12]. Although such analysis ignores the lateral geometry issues it gives a qualitative description within an order of magnitude estimate. Even for Schottky barriers as thin as the ones considered here, and for non-degenerate semiconductors, the effective conductance  $G_{sc}=\sigma_{sc}/L_{sc}$  is much higher than  $G_b$ . The calculation gives, to the lowest order in  $G_b/G_{sc}$ ,  $MR \sim \alpha^2 \frac{G_b}{G_{sc}} \frac{L_{sc}}{d} \frac{f}{f+1}$ . In the two-terminal case the difference between P and AP configurations is accommodated by different non-equilibrium spin-density profiles, with a very small change in the total current. Although  $J^P \simeq J^{AP}$ , the electrochemical potential splitting  $\Delta\mu = |\mu_+^{SC} - \mu_-^{SC}|$  near the contact follows the ratio:

$$\frac{\Delta\mu^P}{\Delta\mu^{AP}} \propto \left( \frac{d}{2L_{sc}} \right)^2 \ll 1, \quad (3)$$

whereas the mean value of  $\mu_s$  does not change visibly between P and AP. Our three terminal scheme makes effective use of Eq. (3).

For a certain ratio  $V_R/V_L$ , the right contact current in the P configuration can be quenched ( $J_R^P = 0$ ), while the AP current remains finite. Thus, the readout of the

magnetic configuration is digitized. From simple circuit theory, when the barrier resistances dominate, the voltage ratio  $V_R/V_L$  which quenches  $J_R^P$  is estimated to be  $1/(rf+1)$ , where  $r$  is the ratio of source to drain widths. We examine the tolerance to error or noise by varying this ratio by  $\pm 0.2\%$ , consistent with the Johnson noise for the barrier resistance with contact area of  $1 \mu\text{m}^2$  at sub-GHz frequencies. Fig. 2 shows the noise margins for the right terminal current as function of the width of the source contact  $w_s$ . For large source width, equivalent to uncoupled spin valves, the MR amplification effect is lost. For ultra-narrow contacts the effect is also small due to the increased resistance of the contact [11]. In-between there is an optimal value of  $w_s$  (well below  $L_{sc}$ ) where the MR effect measured in the right contact easily exceeds hundreds of percent. The resulting current densities calculated at room temperature are of the order of  $1 \text{ A/cm}^2$ , which could be directly measured in sub-micron contacts or further amplified, leading to a robust read-out of the left drain magnetization direction. During the read-out the left contact current density is about  $100 \text{ A/cm}^2$  for the voltages used in Fig. 2.

The amplification of the MR effect depends on the robustness of a finite current  $J_R^{AP}$  when the magnetic configuration is changed to AP. An explanation based on our calculation is as follows. The source of the different currents is the difference in the spin splitting of the electrochemical potential,  $\Delta\mu$ , at the R contact in the P and AP configurations at the optimal voltage ratio. In P,  $\Delta\mu^P$  is small. In AP,  $\Delta\mu^{AP}$  is large, for the reason in Eq. (3), which still qualitatively holds in the MCT. This disrupts the balance of the spin currents on two sides of the source, resulting in a sizable current,  $J_R^{AP} \sim (G_+ - G_-)\Delta\mu^{AP}$ . In the semiconductor channel, the electrochemical potential of one spin population rises a good fraction above  $-eV_R$  and the other one drops an equal amount below. Thus, the current is fully spin-polarized. Fig. 3 shows the two dimensional spatial distribution of the  $x$ -component current densities in the semiconductor channel in the 100 nm section left of the right contact. The middle contact width is at the optimal value shown in Fig. 2. Note that the difference in total current densities between Figures 2 and 3 comes from the ratio of channel thickness  $h$  and R contact width  $w$ . In Fig. 3, the zero and  $4 \text{ A/cm}^2$  respective values in the middle of the color scale for the left and the right upper panels show the zero current in P and a robust finite current in AP. The amplification of the spin current from P to AP is visible in the lower panels. By adding and subtracting the current densities in the upper and lower panels of each column, one can see that the spin currents in the P case flow in the opposite directions at the opposite edges of the channel, resulting in the zero net charge current.

In practical designs, the “soft” L contact might have different properties from the remaining two. The exact

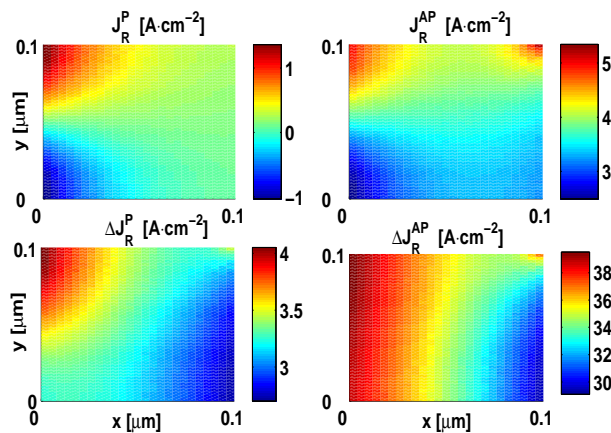


FIG. 3: (color). Spatially resolved  $x$  component of the current density at the right half of the right channel. Note the different scales for each figure. The upper panels show the zero and finite net charge currents for the parallel and antiparallel configurations, respectively (0 versus  $\sim 3.5 \text{ A cm}^{-2}$ ). The lower panels show the amplification of  $\Delta J = j_+ - j_-$  due to the difference in electrochemical potential splitting. The parameters are as in Fig. 2 with optimal source width and  $\tau_{sp} = 80$  ps.

left-right symmetry is not required for the digital effect; any asymmetry between the terminals can be counteracted by adjusting the voltages. Moreover, the zero current state can be stabilized using the feedback loops adjusting  $V_L$  and  $V_R$ . Although the current from the L contact is larger than the read-out R current, the L output needs not be wasted. It can, for instance, be used to amplify the output from the R contact using external circuits.

In all the modeling presented we have used experimentally available properties of FM/SC structures. The formalism and ideas used here can be applied as well to an all-metallic system, with a paramagnetic metal channel. However, vastly different parameters makes the control of the MR amplification effect more difficult. The requirements of having a sizable AP electrochemical potential splitting, of being able to control the voltages with desired accuracy, and of keeping the current densities at reasonable levels, are hard to reconcile. Thus, the semiconductor-based system is more naturally suited for demonstration of voltage-controlled spin transference.

In summary, we have constructed a room temperature theory of the transference of the spin polarization in the current between a pair of electrodes to another pair provided they are connected by spin diffusion. The three-terminal structure effectively exploits the spin accumulation in the semiconductor channel. One result, the amplification of the magneto-resistive effect by voltage control, may be of practical importance as the electrical read-out of magnetic memory integrable to an electronics circuit. Such a device may be used in a scheme of “mag-

netic computation”, working as a building block of reprogrammable logic gate [22]. Such a synergy of information processing and non-volatile storage represents a possible fulfillment of the promises of spintronics. Further properties which may result from the spin transference need to be explored in the future.

This work is supported by NSF under Grant No. DMR-0325599.

---

\* Electronic address: hdery@ucsd.edu

- [1] M. N. Baibich *et al.*, Phys. Rev. Lett. **61**, 2472 (1988).
- [2] G. Binasch, P. Grünberg, F. Saurenbach, and W. Zinn, Phys. Rev. B **39**, R4828 (1989).
- [3] J. S. Moodera, L. R. Kinder, T. M. Wong, and R. Meservey, Phys. Rev. Lett. **74**, 3273 (1995).
- [4] G. A. Prinz, Science **282**, 1660 (1998).
- [5] S. A. Wolf *et al.*, Science **294**, 1488 (2001).
- [6] I. Žutić, J. Fabian, and S. D. Sarma, Rev. Mod. Phys. **76**, 323 (2004).
- [7] A. T. Hanbicki *et al.*, Appl. Phys. Lett. **80**, 1240 (2002).
- [8] A. T. Hanbicki *et al.*, Appl. Phys. Lett. **82**, 4092 (2003).
- [9] X. Jiang *et al.*, Phys. Rev. Lett. **94**, 056601 (2005).
- [10] C. Adelmann, X. Lou, J. Strand, C. J. Palmstrom, and P. A. Crowell, Phys. Rev. B **71**, 121301(R) (2005).
- [11] A. Fert and H. Jaffrès, Phys. Rev. B **64**, 184420 (2001).
- [12] E. I. Rashba, Eur. Phys. J. B **29**, 513 (2002).
- [13] S. Datta and B. Das, Appl. Phys. Lett **56**, 665 (1990).
- [14] C. Ciuti, J. P. McGuire, and L. J. Sham, Appl. Phys. Lett **81**, 4781 (2002).
- [15] I. Žutić, J. Fabian and S. DasSarma, Phys. Rev. Lett. **88**, 066603 (2002).
- [16] M. E. Flatté, Z. G. Yu, E. Johnston-Halperin and D. D. Awschalom, Appl. Phys. Lett **82**, 4740 (2003).
- [17] J. Schliemann, J. C. Egues and D. Loss, Phys. Rev. Lett. **90**, 146801 (2003).
- [18] S. A. Crooker and D. L. Smith, Phys. Rev. Lett. **94**, 236601 (2005).
- [19] J. Stephens, J. Berezovsky, J. P. McGuire, L. J. Sham, A. C. Gossard, D. D. Awschalom, Phys. Rev. Lett. **93**, 097602 (2004).
- [20] F. J. Jedema, A. T. Filip, and B. J. van Wees, Nature **410**, 345 (2001).
- [21] M. Johnson, Science **260**, 320 (1993).
- [22] A. Ney, C. Pampuch, R. Koch, and K. H. Ploog, Nature **425**, 485 (2003).
- [23] S. Hershfield and H. L. Zhao, Phys. Rev. B **56**, 3296 (1997).
- [24] Z. G. Yu and M. E. Flatté, Phys. Rev. B **66**, 235302 (2002).
- [25] E. I. Rashba, Phys. Rev. B **62**, R16267 (2000).
- [26] J. D. Albrecht and D. L. Smith, Phys. Rev. B **68**, 035340 (2003).
- [27] *Tunneling Phenomena*, edited by E. Burnstein and S. Lundqvist (Plenum Press, New York, 1969).
- [28] W. H. Butler *et al.*, J. Appl. Phys. **81**, 5518 (1997).
- [29] *Optical Orientation*, edited by F. Meier and B. P. Zakharchenya (Nort-Holland, New York, 1984).